The effects of thermal sources on natural convection in an enclosure

Heiu-Jou Shaw*
Department of Naval Architecture and Marine Engineering

Cha'o-Kuang Chen†
Department of Mechanical Engineering, National Cheng-Kung University, Tainan, Taiwan, Republic of China

J. W. Cleaver‡
Department of Mechanical Engineering, University of Liverpool, UK

Received March 1987 and accepted for publication July 1987

In this paper, the phenomena of natural convection in an enclosure with isolated thermal sources located on a vertical adiabatic surface is investigated numerically. The arrangement of the problem is pertinent to the positioning of the thermal sources in a container. Flow patterns and temperature profiles in the enclosure and average heat transfer rates on the boundary surfaces are evaluated by a cubic spline collocation method for various thermal sources arrangements and Rayleigh number. It is obvious that the fluid flow and heat transfer in the enclosure is affected strongly by the arrangement of the thermal sources.

Keywords: natural convection; numerical computation

Introduction

Owing to the rapid development of the semiconductor, electronic equipment is widely applied to human life and military use. The natural convection cooling problem for electronic equipment with thermal sources is a very common and desirable method for removing heat from the equipment. The application of natural convection cooling for electronic equipment ranges from individual transistors to mainframe computers and from power supplies to telephone switchboards. Natural convective cooling is maintenance free, requires no energy supply, and is safe.

The problem of natural convection induced by isolated thermal sources on a vertical surface has been the subject of many studies. Recently, Jaluria[1-3] studied numerically the interaction of natural convection wakes arising from thermal sources on a vertical surface in an open region. The effects of the thermal sources location and size have been studied by Sparrow[4], Chu, Churchill, and Patterson[5], Clomburg[6], and Acharya and Goldstein[7]. The wall plumes due to finite-sized thermal sources have also been investigated numerically and experimentally[8,9].

For practical applications, the present study considers the natural convective cooling due to the thermal sources on a vertical board, which is fitted with an enclosure. In this study, the influence of the location of the thermal sources on the flow field and heat transfer rate has been determined.

Mathematical formulation

The configuration and coordinate system of the problem are given in Figure 1. The two-dimensional square cavity is fitted with thermal sources and an adiabatic board. Two finite-sized thermal sources of heights E_1 and E_2, separated by a distance B, is located on one of the vertical surfaces of the adiabatic surface. The thermal sources are of constant temperature T_s. The bottom wall of enclosure is insulated while the other walls are maintained at a uniform temperature T_0.

The vorticity and stream function are used to eliminate pressure as a variable and to eliminate the need for the direct inclusion of the continuity equation in the investigation. The resulting governing equations are

$$\frac{\partial T^*}{\partial \tau} + U\frac{\partial T^*}{\partial X} + V\frac{\partial T^*}{\partial Y} = \nabla^2 T^* \tag{1}$$

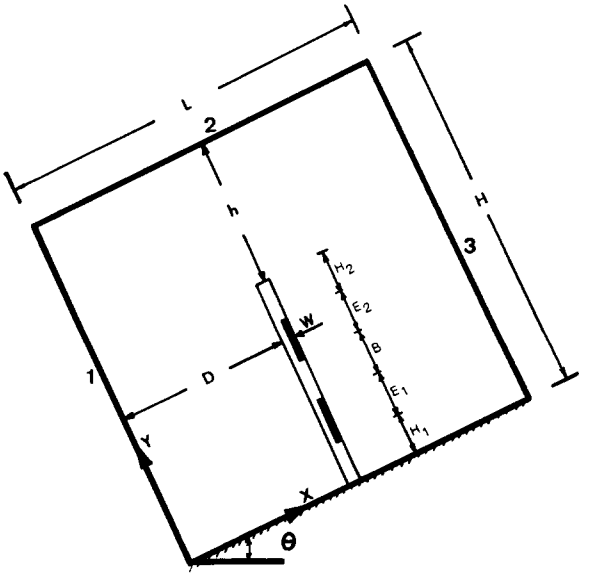

Figure 1 Physical model

* Lecturer.
† Professor.
‡ Senior lecturer.

$$\frac{\partial\Omega}{\partial\tau}+\frac{\partial(U\Omega)}{\partial X}+\frac{\partial(V\Omega)}{\partial Y}$$
$$=\mathrm{Ra}\,\mathrm{Pr}\left(\frac{\partial T^*}{\partial X}\cos\theta-\frac{\partial T^*}{\partial Y}\sin\theta\right)+\mathrm{Pr}\,\nabla^2\Omega \quad (2)$$

$$\Omega=-\nabla^2\Psi \quad (3)$$

$$U=\frac{\partial\Psi}{\partial y},\qquad V=-\frac{\partial\Psi}{\partial x} \quad (4)$$

The dimensionless variables $X=x/L$, $Y=y/L$, $\tau=t/(L^2/\alpha)$, $U=u/(\alpha/L)$, $\Omega=\omega/(\alpha/L^2)$, $\Psi=\psi/\alpha$, and $T^*=(T_s-T_0)/T_0$ represent the dimensionless coordinates, time, velocity, vorticity, stream function, and temperature, respectively.

The boundary conditions are

$$X=0,1,\qquad T^*=0,\quad U=V=0$$

$$Y=\frac{H}{L},\qquad T^*=0,\quad U=V=0$$

$$Y=0,\qquad \frac{\partial T^*}{\partial Y}=0,\quad U=V=0$$

$$X=\frac{D}{L},\quad 0\leqq Y\leqq\frac{H-h}{L},\quad \frac{\partial T^*}{\partial X}=0,\quad U=V=0$$

$$X=\frac{D+W}{L},\quad 0\leqq Y\leqq\frac{H_1}{L},\quad \frac{\partial T^*}{\partial X}=0,\quad U=V=0$$

$$X=\frac{D+W}{L},\quad \frac{H_1}{L}\leqq Y\leqq\frac{H_1+E_1}{L},\quad T^*=1,\quad U=V=0$$

$$X=\frac{D+W}{L},\quad \frac{H_1+E_1}{L}\leqq Y\leqq\frac{H_1+E_1+B}{L},\quad \frac{\partial T^*}{\partial X}=0,\quad U=V=0 \quad (5)$$

$$X=\frac{D+W}{L},\quad \frac{H_1+E_1+B}{L}\leqq Y\leqq\frac{H_1+E_1+B+E_2}{L},\quad T^*=1,\quad U=V=0$$

$$X=\frac{D+W}{L},\quad \frac{H_1+E_1+B+E_2}{L}\leqq Y\leqq\frac{H_1+E_1+B+E_2+H_2}{L},\quad \frac{\partial T^*}{\partial X}=0,\quad U=V=0$$

$$Y=\frac{H-h}{L},\quad 0<X<\frac{D+W}{L},\quad \frac{\partial T^*}{\partial Y}=0,\quad U=V=0$$

In the above equations, two governing parameters appear: the Prandtl number ($\mathrm{Pr}=\nu/\alpha$) and the Rayleigh number ($\mathrm{Ra}=\beta g L^3 T_m/\nu\alpha$). In this study, the Prandtl number is assigned a value of 1.0.

The overall heat transfer rates for the boundaries of the enclosure are defined as

$$\mathrm{HTR}_1=\int_0^1\left[\frac{\partial T^*}{\partial X}\right]_{X=0}\mathrm{d}Y$$
$$\mathrm{HTR}_2=\int_0^1\left[\frac{\partial T^*}{\partial Y}\right]_{Y=1}\mathrm{d}X \quad (6)$$
$$\mathrm{HTR}_3=\int_0^1\left[\frac{\partial T^*}{\partial X}\right]_{X=1}\mathrm{d}Y$$

The numerical integration of Equation 6 was performed after the steady-state temperature field was obtained.

Numerical procedure

The coupled equations (1)–(3) were discretized by using the cubic spline collocation formulation[10]. The spline alternating direction implicit procedure (SADI) was applied to perform the numerical computation[10-13]. Details of the SADI procedure are given in Ref. 10. The interior grid lines were spaced nonuniformly in both the x- and y-directions. We employ a nonuniform grid with a smaller spacing of the mesh points in the neighborhood of the boundary. The grid fineness $m\times n$ (35×35) was found adequate to provide accurate results for the present problem. The numerical procedure is described as follows:

(0) Determine the time step.
(1) Start with solving the energy equation (1).
(2) Compute the boundary values of vorticity and solve the vorticity equation (2).
(3) Solve the stream function equation (3) by using the false transient technique[10], until convergence is achieved; i.e.,

$$\left|\frac{\Psi_{ij}^s-\Psi_{ij}^{s-1}}{\Psi_{\max}^s}\right|<10^{-4} \quad (7)$$

where s denotes the number of the false time step.
(4) Repeat steps (1)–(3) until the maximum relative change in temperature and flow fields satisfies the criterion

$$\left|\frac{\phi_{ij}^z-\phi_{ij}^{z-1}}{\phi_{\max}^z}\right|<10^{-4} \quad (8)$$

where ϕ refers to Ψ, θ, Ω, and z denotes the number of time steps. When the process has converged, the steady-state condition is reached.

Results and discussions

The plots of the flow pattern, streamlines, and isotherms as well as the average heat transfer rate along the isothermal walls of the enclosure are presented.

Nomenclature

u, U	Dimensional and dimensionless horizontal velocity
v, V	Dimensional and dimensionless vertical velocity
x, X	Dimensional and dimensionless horizontal coordinate
y, Y	Dimensional and dimensionless vertical coordinate
α	Fluid thermal diffusivity
β	Coefficient of thermal expansion
μ	Viscosity
ν	Kinematic viscosity, μ/ρ
ρ	Density
ψ, Ψ	Dimensional and dimensionless stream function
θ	Orientation of the enclosure
τ	Dimensionless time
ω, Ω	Dimensional and dimensionless vorticity

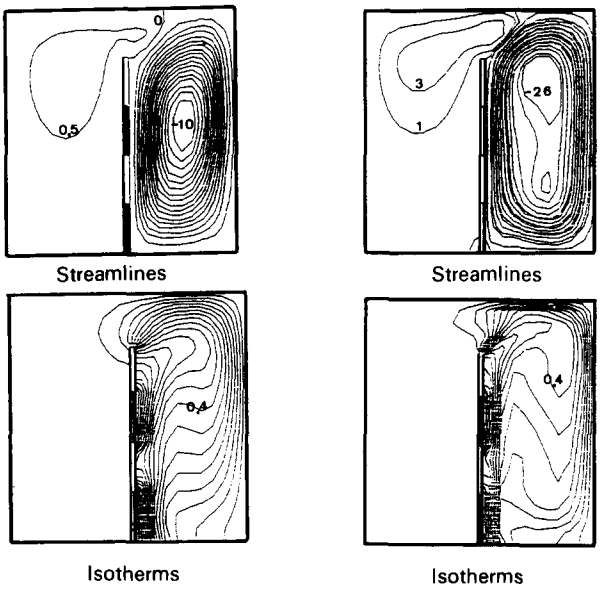

Figure 2 Streamlines and isotherms for a square enclosure with thermal sources at Pr=1, $D/L=0.5$, $W/L=0.025$, $E_1/L=E_2/L=0.2$, $B/L=0.2$, $H_1/L=0.0$, $H_2/L=0.2$ and (a) $Ra=10^5$, (b) $Ra=10^6$

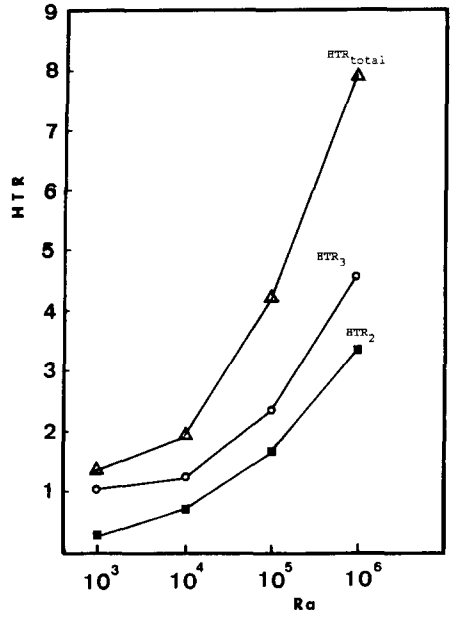

Figure 3 Effects of Rayleigh number on average heat transfer rate

Effect of the Rayleigh number on enclosure

The streamlines and isotherms for a square enclosure with an adiabatic board and thermal sources, with $Ra=10^5$ and 10^6, are shown in Figure 2.

From Figure 2, it can be seen that there is no streamline or isotherm in the zone between the left wall and the adiabatic board. Accordingly, there exists no natural convection in this zone, and the heat transfer rate of the left wall can be neglected. The effect of the Rayleigh number on the average heat transfer rate is given in Figure 3. In Figure 3, both the average heat transfer rate on the right and top walls increase as the Rayleigh number increases. Accordingly, the total transfer rate increases significantly.

Effect of the orientation of the enclosure with thermal sources

The flow patterns and temperature distributions for various orientations of the square enclosure with an adiabatic board and thermal sources with $Ra=10^6$ are shown in Figure 4.

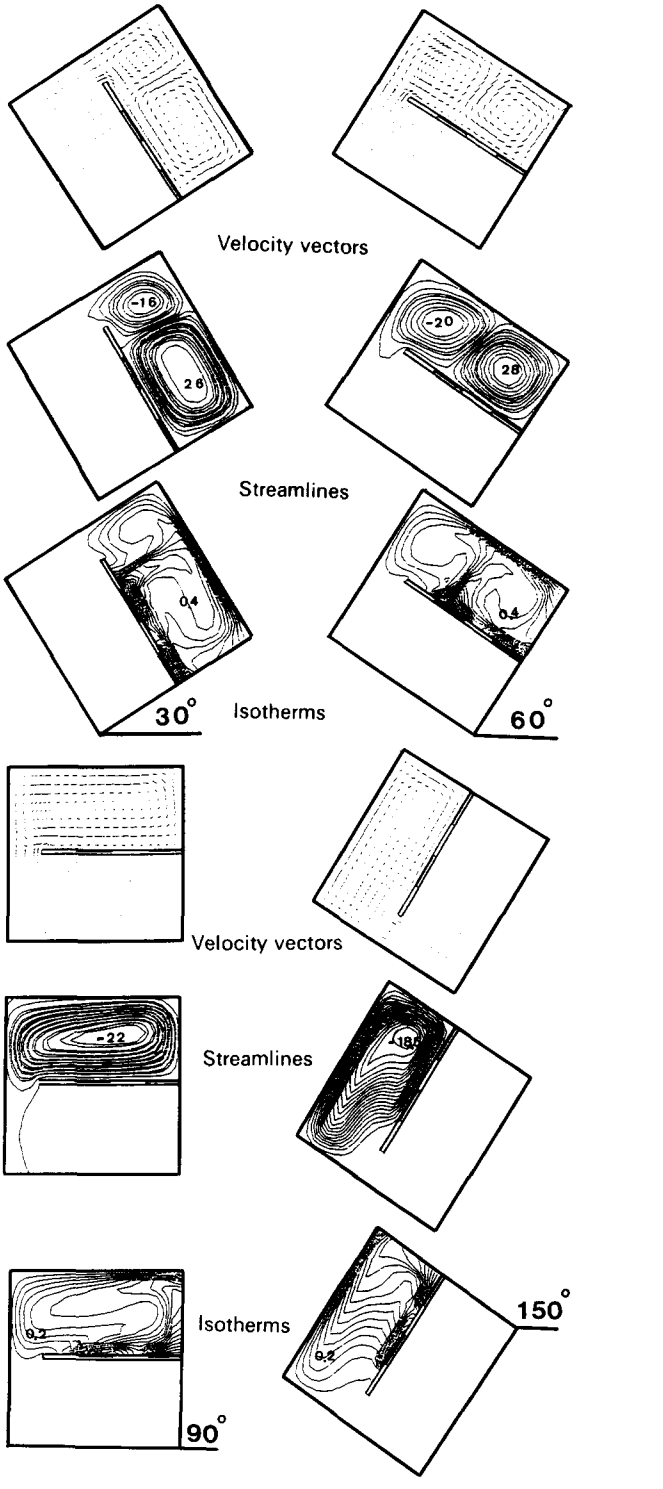

Figure 4 Velocity vectors, streamlines, and isotherms for various orientation of the square enclosure with thermal sources for $Ra=10^6$, Pr=1, $D/L=0.5$, $W/L=0.025$, $E_1/L=E_2/L=0.2$, $B/L=0.2$, $H_1/L=0.0$, $H_2/L=0.2$ at (a) $\theta=30°$, (b) $\theta=60°$, (c) $\theta=90°$, (d) $\theta=150°$

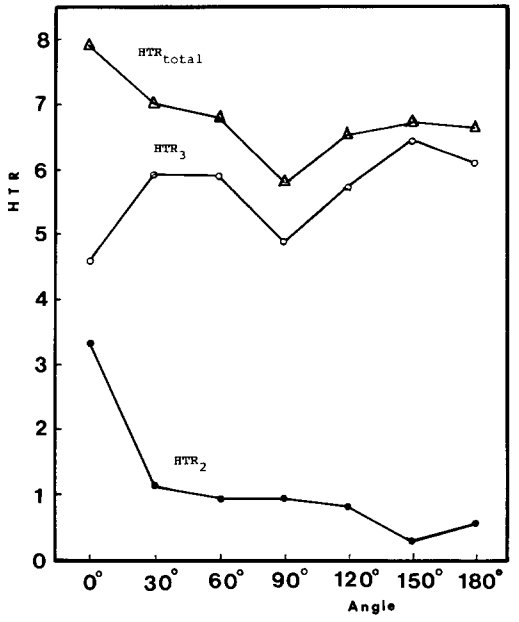

Figure 5 Effects of orientation of the square enclosure on average heat transfer rate

Comparisons of the variation of heat transfer rate due to different orientations of the square enclosure with thermal sources are given in Figure 5. It is shown that the heat transfer rate on the top wall of the enclosure is decreasing when the angle of the orientation is increasing. However, the effect of heat transfer rate on the right wall (HTR_3) increases until the enclosure is inclined to 30°; it then decreases and reaches the worst condition at 90°. The top curve represents the total heat transfer rate. The best heat transfer condition is when the enclosure is not inclined, and the worst heat transfer condition is when the inclination of the enclosure reaches 90°.

Effect of the location of adiabatic board with thermal sources

The streamlines and isotherms for a square enclosure with an adiabatic board and thermal sources at different locations ($D/L=0.2$ and 0.8) in a given condition are shown in Figure 6(a), (b). The farther the distance between the adiabatic board and left wall is, the denser the isotherms for the zone near the right wall will be.

The effects of location of the adiabatic board and orientation of the enclosure on average heat transfer rate are given in Figure 7. HTR_3 obviously increases, but HTR_2 on the top wall 2 decreases, as the distance increases between the adiabatic board and left wall. However, the total heat transfer rate varies slightly when the enclosure is inclined from the right position to 30° for the different locations ($D/L=0.2$, 0.5, and 0.8) of the adiabatic board. As the enclosure is inclined from 30° to 60°, the total heat transfer rate for $D/L=0.2$ decreases significantly due to the reversal flow between the adiabatic board and the right wall of the enclosure. It can be seen that the total heat transfer rate is in its best condition at $D/L=0.5$. As $D/L=0.2$, the total heat transfer rate becomes the worst one. It is clear that increasing the value of the distance between the adiabatic board and left wall results in a significant increase of HTR_3 and a significant decrease of HTR_2. Increasing D/L does not significantly increase the total average heat transfer rate ($HTR_{total}=HTR_2+HTR_3$).

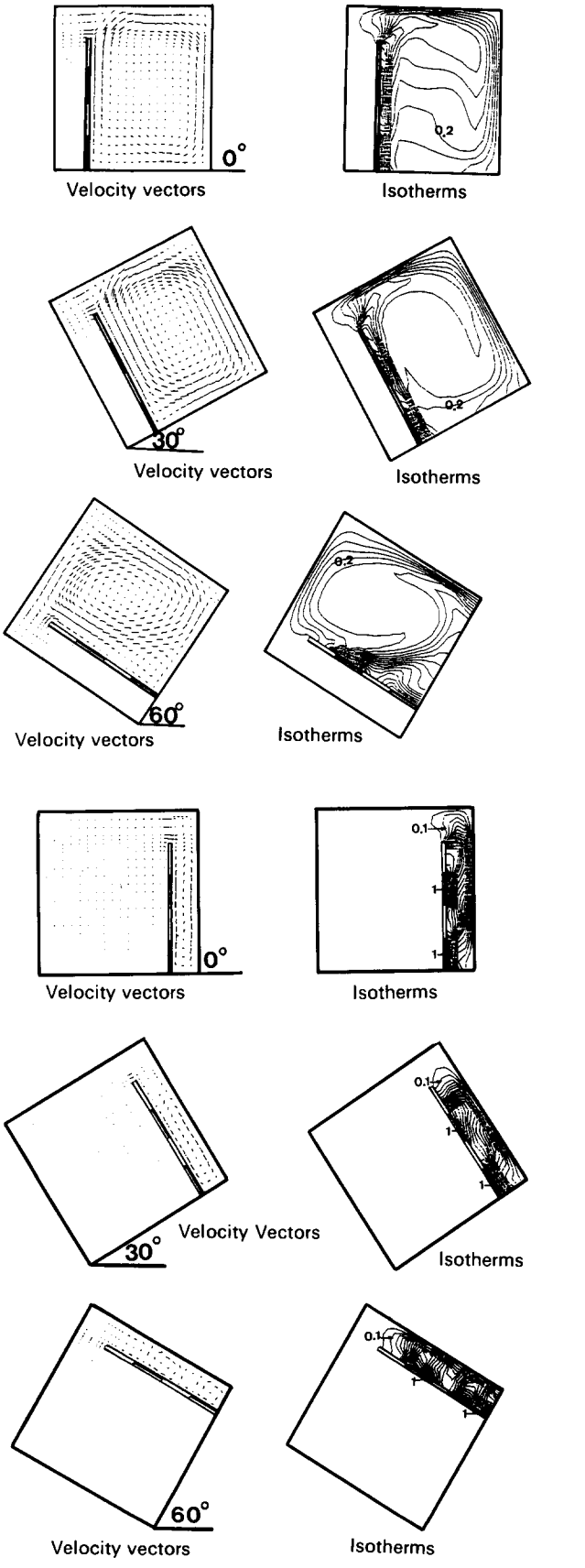

Figure 6 Velocity vectors and isotherms for various orientations of the square enclosure with adiabatic board and thermal sources for $Ra=10^6$, $Pr=1$, $W/L=0.025$, $E_1/L=E_2/L=0.2$, $B/L=0.2$, $H_1/L=0.0$, $H_2/L=0.2$ at (a) $D=0.2$, (b) $D=0.8$

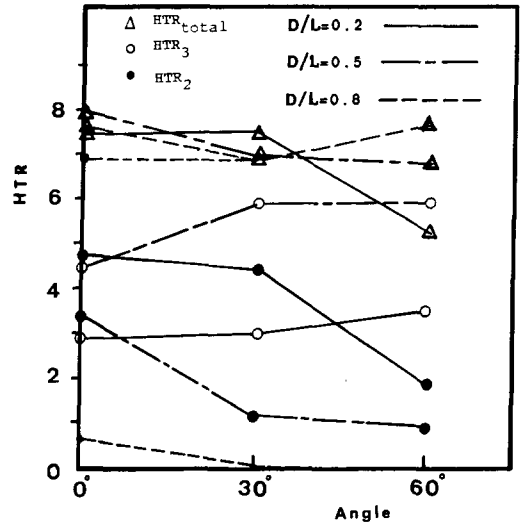

Figure 7 Effects of the location of the adiabatic board and orientation of the enclosure on average heat transfer rate

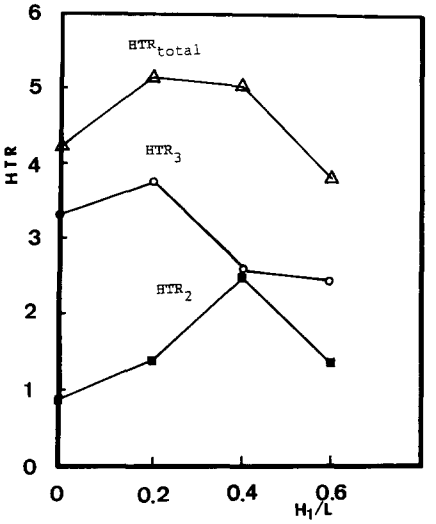

Figure 9 Effects of the thermal source location on average heat transfer rate

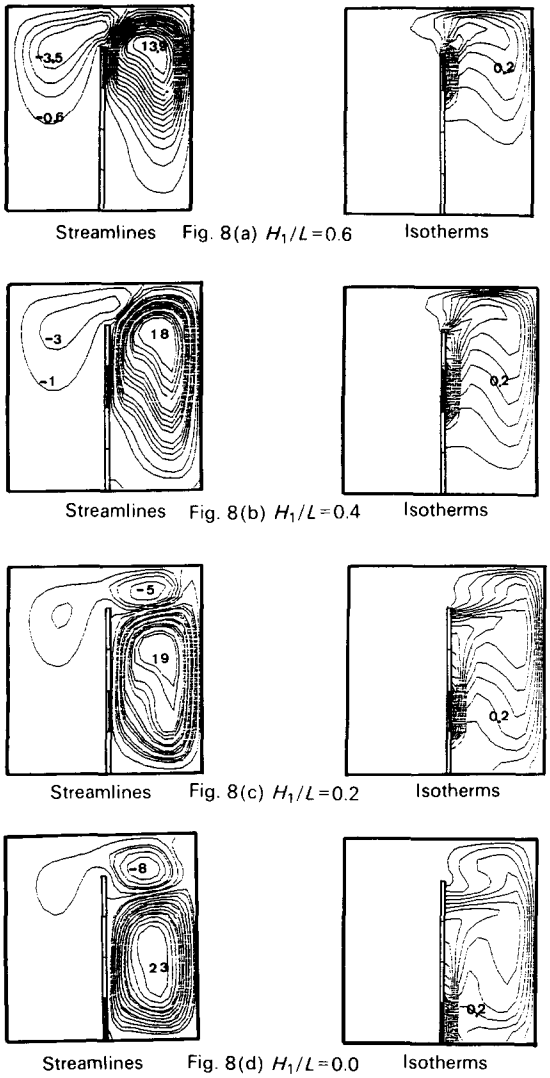

Figure 8 Streamlines and isotherms for a square enclosure with a thermal source on an adiabatic board at different location for Ra=10^6, Pr=1, D/L=0.5, W/L=0.025, E_1/L=0.2, E_2/L=0.0 for H_1/L equal to (a) 0.6, (b) 0.4, (c) 0.2, (d) 0.0

Effect of the location of thermal sources on an adiabatic board

For a given thermal source size on a vertical adiabatic board, the effect of the location of the thermal source can be studied by moving the thermal source up and down while keeping the board in the same location. The computed velocity vectors, streamlines, and isotherms in the enclosure with Ra = 10^6 and $E_1/L=0.2, E_2/L=0.0$ are plotted in Figure 8. Four locations are chosen: $H_1/L=0.0, 0.2, 0.4$, and 0.6, where H_1/L is the distance between the bottom of the thermal source and the surface of the bottom wall. The effects of H_1/L on the average heat transfer rate are given in Figure 9. It is obvious from Figure 8 that increasing H_1/L causes upward movement of the streamlines and isotherms until they are restrained by the top wall. Figure 9 shows how the different locations of the thermal sources will affect the average heat transfer rate. The average heat transfer rates on the right wall (HTR_3) and top wall (HTR_2) increase first ($H_1/L=0.0$ to 0.2). As H_1/L increases from 0.2 to 0.4, HTR_3 decreases significantly, but HTR_2 is increasing continuously until $H_1/L=0.6$. Finally, HTR_2 and HTR_3 decrease as H_1/L increases ($H_1/L=0.6$).

Effects of the slit width between the adiabatic board and the top wall of the enclosure

The flow patterns and temperature distributions for various slit widths between the adiabatic board and the top wall of the enclosure for $h/L=0.05, 0.15$, and 0.35 are shown in Figure 10, where h/L is the slit width. It can be observed that the buoyancy flow in the largest slit-width enclosure (Figure 10(a)) exists with a strong secondary flow in the left-hand part of the enclosure. With decreasing slit width (Figure 10(b), (c)), the strength of the secondary flow in the enclosure is reduced. The effect of the slit width between the adiabatic board and the top wall of the enclosure on the average heat transfer rate is shown in Figure 11. It can be seen that the total heat transfer rate will change slightly due to the increase of the slit width; however, the heat transfer rate on the top wall of the enclosure (HTR_2) increases significantly. On the other hand, the heat transfer rate on the right wall of the enclosure first increases and then decreases.

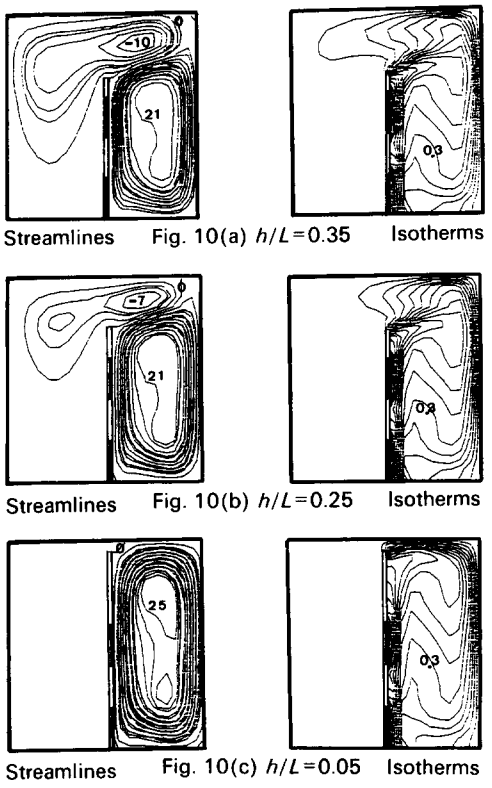

Figure 10 Streamlines and isotherms for a square enclosure with thermal sources on various adiabatic boards for Ra=10^6, Pr=1, D/L=0.5, W/L=0.025, $E_1/L=E_2/L$=0.2, H_1/L=0.0, B/L=0.2 for h/L equal to (a) 0.35, (b) 0.25, (c) 0.05

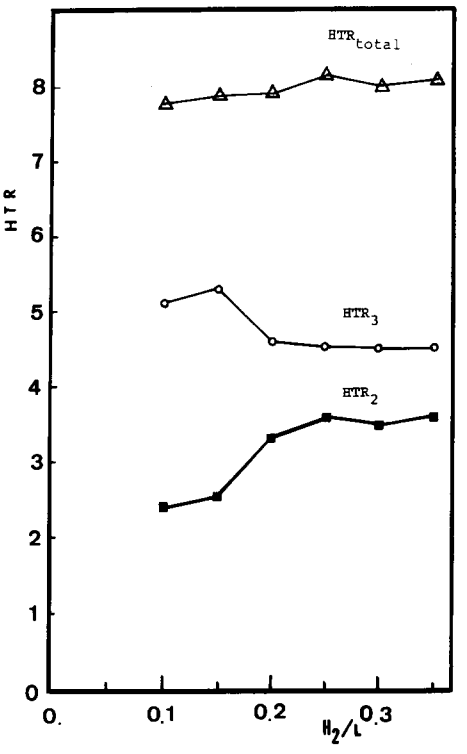

Figure 11 Effects of the width of slit between adiabatic board and top wall of enclosure on average heat transfer rate

Conclusion

The characteristics of natural convection of a square enclosure with thermal sources have been studied numerically. It is found that the Rayleigh number, location of the thermal source, and orientation of the enclosure significantly influence the overall flow and temperature variations in the enclosure. The present numerical study can be used readily to analyze the influence of the important parameters on the fluid flow and temperature variation, such as the Rayleigh number and different arrangement of thermal sources in enclosures.

References

1 Jaluria, Y. and Gebhart, B. Buoyancy-induced flow arising from a line thermal source on an adiabatic vertical surface. *Int. J. Heat Mass Transfer*, 1977, **20**, 153–157

2 Jaluria, Y. Buoyancy-induced flow due to isolated thermal sources on a vertical surface. *J. Heat Transfer*, 1982, **102**, 223–227

3 Jaluria, Y. Interaction of natural convection wakes arising from thermal sources on a vertical surface. *J. Heat Transfer*, 1985, **107**, 883–892

4 Sparrow, E. M. and Faghro, M. Natural convection heat transfer from the upper plate of a colinear, separated pair of vertical plates. *J. Heat Transfer*, 1980, **102**, 623–629

5 Chu, H. H.-S., Churchill, S. W., and Patterson, C. V. S. The effect of heater size, location, aspect ratio, and boundary conditions on two-dimensional, laminar, natural convection in rectangular channels. *J. Heat Transfer*, 1976, **98**, 194–201

6 Clomburg, L. A., Jr. Convection in an enclosure-source and sink located along a single horizontal boundary. *J. Heat Transfer*, 1978, **100**, 205–211

7 Acharya, S. and Goldstein, R. J. Natural convection in an externally heated vertical or inclined square box containing internal energy sources. *J. Heat Transfer*, 1985, **107**, 855–866

8 Gebhart, B., Pera, L., and Schorr, A. W. Steady laminar natural convection plumes about a horizontal line heat source. *Int. J. Heat Mass Transfer*, 1970, **13**, 161–171

9 Sparrow, E. M., Patanker, S. V., and Abdel-Wahed, R. M. Development of wall and free plumes above a heated vertical plate. *J. Heat Transfer*, 1978, **100**, 184–190

10 Rubin, S. G. and Graves, R. A. Viscous flow solution with a cubic spline approximation. *Computers and Fluids*, 1975, **3**, 1–36

11 Rubin, S. G. and Khosla, P. K. Higher-order numerical solutions using cubic splines. *AIAA J.*, 1976, **14**, 851–858

12 Rubin, S. G. and Khosla, P. K. Polynomial interpolation methods for viscous flow calculations. *J. Comput. Physics*, 1977, **24**, 217–244

13 Wang, P. and Kahawita, R. Numerical integration of partial differential equations using cubic splines. *Int. J. Computer Math.*, 1983, **13**, 271–286